Enhanced Kinetics of Enzymatic Nanosensors

Joyce Breger[1,4], Scott Walper[1], Mario Ancona[3], Michael Stewart[2], Kimihiro Susumu[2], and Igor Medintz[1*]
[1]Center for Bio/Molecular Science and Engineering, Code 6900,
[2]Optical Sciences Division, Code 5600,
[3]Electronic Science and Technology Division, Code 6800, U.S. Naval Research Laboratory, Washington, DC 20375,
[4]American Society for Engineering Education, 1818 N Street NW, Suite 600 Washington, DC
*igor.medintz@nrl.navy.mil

ABSTRACT

Nanosensors employing quantum dots (QDs) and functional moieties such as enzymes are promising for diagnostics and chemical/biological threat activity. Their small size permits cell penetration and their inherent photochemical properties are well-suited for rapid, optical measurements. The effectiveness of biorecognition agents immobilized on QDs are not completely understood, hindering development of chemical/biological sensors and remediation materials. We analyze an engineered enzyme construct's effectiveness when attached to QDs illustrating an important biological threat application: neutralization of paraoxon, a simulant nerve agent. Phosphotriesterase trimer (PTE_3) was engineered to contain 3 PTE monomers attaced to a V-domain, collogen linker, and a oligohistidine (His_6) tail. Various ratios of PTE_3 were attached to two sizes of QDs, 525 or 625 nm via metal coordination. Characteristic kinetic parameters of PTE_3-QD were compared to free enzyme.

Keywords: Quantum dots, enzyme, phopsphotriesterase, paraoxon, kinetics

1 INTRODUCTION

As nature's catalysts, enzymes rapidly and efficiently transform numerous chemicals in chemical synthesis far beyond our capabilities. Harnessing enzymes' ability to catalyze chemicals of interest would circumvent creating difficult synthetic processes. Indeed, much effort has been focused in engineering enzymes with modulated activity for a variety of industrial processes.[1, 2] One phenomenon that is poorly understood but has been observed to increase catalytic activity is attaching enzymes to nanoparticles.[3] Understanding how and why enzyme activity increases at the nanoparticle surface could lead to developments in creating microfluidic devices that detect biomarkers or chemical warfare agents.

Nanosensors composed of QDs and functional moieties such as enzymes are promising for disease surveillance/diagnostics and chemical/biological threat activity. Numerous advantages of QDs over other nanoscaffolds include their inherent photochemical properties such as size tunable fluorescence, ease in attaching functional moieties, resistance to photobleaching, and much more making QDs well-suited for rapid, optical measurement applications.[4] Their small size also permits cell penetration which might be useful in theranostic application development.[5]

PTE catalyzes the detoxification of organophosphate pesticides to *p*-nitrophenol. To elucidate the mechanisms that increase catalytic activity of enzymes attached to nanoparticles, we attached various ratios of PTE_3 to two distinctly sized QDs, 525 or 625 nm and study the kinetics of hydrolyzing paraoxon.

2 METHODS

2.1 Quatum Dots

Green and red emitting CdSe/Zns (core/shell) QDs whose emission was centered at ca. 525 and 625 nm were synthesized and solubilized with dihydroplipoic acid-based zwitterionic compact ligand (DHLA-CL4) as described elsewhere.[6] DHLA-CL4 renders the QDs biocompatible with high quantum yields and long term stability in a broad pH range (pH = 5-13) while still allowing the QD surface to be functionalized with a variety of biologicals through either covalent attachment or metal affinity coordination.[7, 8] QDs functionalize with these ligands have already proven themselves in a variety of challenging environments.[9-11]

2.2 Phosphotriesterase Trimer Enzyme Preparation

The PTE_3 was engineered by combining the phosphotriesterase gene from Brevundimonas diminuta [12] with the collagen-like triple helix domain and the trimerization V domain from Streptococcus pyogenes. [13, 14] The PTE_3 cassette was excised from a maintenance plasmid and cloned to the bacterial expression vector pET28 (Stratagene) via a NcoI/NotI restriction enzyme digest. The pET28 vector allowed for controlled protein expression and integration of a C-terminal hexa-histidine which could be employed for subsequent immobilized metal affinity

chromatography and QD assembly. The expression construct's sequence was confirmed prior to transformation into the Escherichia coli BL21 (DE3) expression strain. Protein was expressed and purified using shake flask cultures, typically yielding ~10 mg of protein per liter of cell culture. While spontaneous, trimer formation was not immediate, therefore, purified monomeric protein (Mw~53 kDa) was incubated at 4°C for 48 h to allow the triple helix PTE_3 tertiary structure (Mw ~160 kDa) to form. The trimer was isolated from the monomers and dimers by size exclusion chromatography. The gene sequence, description of the protein engineering and purification are described elsewhere. [15]

2.3 Phosphotriesterase Trimer-QD Bioconjugate Assemblies

QDs were diluted to a final concentration of 2.22 nM in 150 μM (pH = 8) CHES buffer and molar equivalents of PTE_3 were added at the indicated ratios while maintaining the final volume of each reaction at 1350 μL within 2 mL Eppendorf tubes. The solutions were vortexed and microcentrifuged briefly to ensure solution homogeneity. Enzyme control reactions contained no QD and only equivalent concentrations of PTE_3.

2.4 PTE Trimer Enzymatic Assays

PTE_3-QD bioconjugate activity was monitored using a Tecan Infinite M1000 dual monochromator multifunction plate reader equipped with a xenon flash lamp (Tecan, Research Triangle Park, NC). Hydrolysis of paraoxon in the presence of PTE_3-QD or PTE_3 free in solution was monitored over time by measuring the absorbance at 405 nm every 20 seconds while maintaining the temperature at 25°C. To a 384-well Corning flat bottom, non-binding plate, 10 μL of free PTE_3 or PTE_3-QD bioconjugate was pipetted into each well. A serial dilution of paraoxon solution was made in CHES buffer ranging in concentration from 5000 to 20 μM in a separate 96-well plate. Right before the start of the experiment, 10 μL of the serially diluted paraoxon was added to each well of the 384-well plate. Absorbance values were converted to concentrations values using a standard curve of *p*-nitrophenol. Initial rates were determined using a macro written in excel with an R^2 value=0.995. Kinetic parameters were determined by fitting the initial rates to the Micheales-Menten equation (1) by minimizing the error between the estimated initial rates and the actual rates.

$$\frac{dP}{dt} \cong -\frac{d[S]}{dt} = \frac{V[S]}{K_M + [S]}, k_{cat} = \frac{V_{max}}{[E]_o} \quad (1)$$

2.5 Agarose Gel Electrophoresis

PTE_3 was allowed to self-assemble onto 525 nm QDs at increasing stoichiometric ratios (0 to 16 per QD).[15] Each reaction contained 5 picomoles of QD at a final volume of 20 μL and was incubated at room temperature for 30 min to facilitate assembly. The assemblies were run on a precast 1.5% agarose low electroendosmosis (EEO) gel in 1X Tris-Borate-EDTA buffer at pH = 8.3. The gel was visualized with a BioRad Gel Image Analyzer to monitor QD migration.

2.6 Dynamic Light Scattering and ζ-potential

Dynamic light scattering (DLS) measurements were carried out using a CGS-3 goniometer system equipped with a single-photon counting avalanche photodiode for signal detection (ALV, Langen, Germany) and analyzed using Dispersion Technology Software (DTS, Malvern Instruments Ltd, Worcestershire, UK).[16, 17] The data of the pre-filtered QDs (with 0.25 μm Millipore syringe filters for typically ~ 1μM) was repeatedly collected (3-5 times) at 20°C and the number profile versus hydrodynamic size was used for data presentation. For Zeta-Potential (ζ-potential) measurement, Laser Doppler Velocimetry (LDV) measurements were performed using a ZetaSizer NanoSeries (Malvern Instruments Ltd, Worcestershire, UK) at 25°C. Three runs of the measurements were performed for each sample prepared in 0.1×PBS buffer at pH 7.4.

3 RESULTS

In this work, we attempt to elucidate the mechanisms for enhanced catalytic activity when enzymes are attached to nanoparticle surfaces as compared to free enzyme in solution. Figure 1 schematically shows the ribbon and stick model of PTE_3 composed of His_6 tail, triple helix domain, V stabilization domain, linker sequence, and PTE monomer and how the assembly would attach to the QD surface.

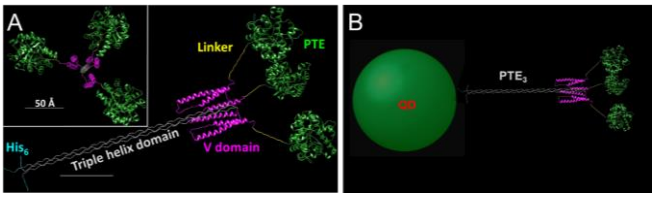

Figure 1. (A) Ribbon and stick model of PTE_3 composed of His-6 tail, triple helix domain, V stabilization domain, linker sequence, and PTE monomer. Scale bar = 5 nm (B) Schematic demonstrating PTE_3 assembly onto QD relative to scale. Adapted from Ref [15] with permission of the Royal Society of Chemistry.

To confirm PTE_3 attached to the QD surface through metal coordination, increasing discrete ratios of PTE_3 were assembled to QD and performed an agarose gel, DLS and measured the ζ-potential. The diameters of the green and red QDs were determined to be 4.3 ± 0.5 and 9.2 ± 0.8 nm, respectively corresponding to surface areas of ~58 and ~266 nm^2.[15, 18] As shown in Figure 2 A, the electrophoretic mobility shift assay (EMSA) demonstrates as the ratio of PTE_3 assembled to QD increases, the mobility of the assemblies decreases; indicating an overall increase in the

MW of the assemblies. Arrows indicate the smallest and highest ratios of assembled PTE_3/QD. DLS confirmed bioconjugates spontaneously self-assemble as shown in Figure 2 B by the increasing hydrodynamic diameter with increasing PTE_3/QD ratio. The constructs were engineered to have the $(His)_6$ tail distally located from the enzyme therefore more than two times the maximum of 12 or 24 dimeric PTE to 525 or 625 nm QDs respectively could be assembled to the QD surface. Also, the enzyme binding pocket should face outward and not be sterically hindered.

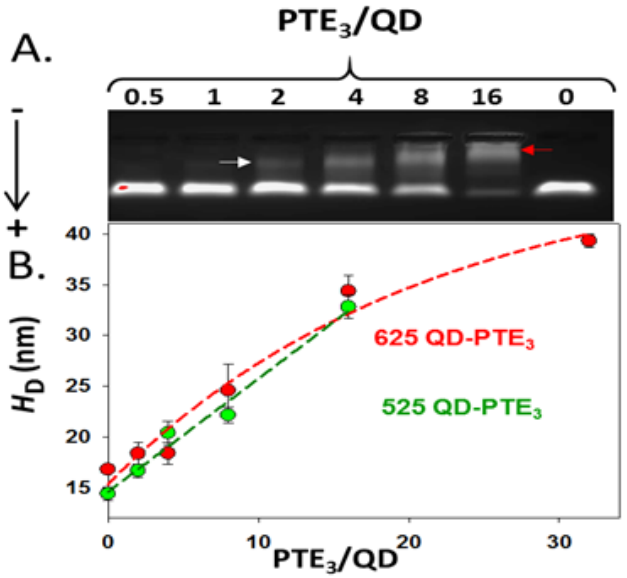

Figure 2. (A) Representative gel of increasing ratios of PTE3 assembled to 525 nm QDs. (B) Hydrodynamic diameter (H_D) determined by DLS for increasing ratios of PTE3 attached to either 525 or 625 nm QD. Adapted from Ref. [15] with permission of the Royal Society of Chemistry.

Significant enhancement in activity was seen when PTE_3 attached to either 525 nm or 625 nm QDs as compared to free enzyme at each of the ratios tested (Figure 3). Paraoxon is an insecticide and an organophosphate stimulant therefore it is commonly used as substrate for studying this family of enzymes. PTE hydrolyzes paraoxon to *p*-nitrophenol whose absorbance can be monitored overtime at 405 nm. Characteristic kinetic parameters were determined by fitting the Michaelis–Menten equation (Equation 1) to the initial rates versus paraoxon concentrations for each ratio of PTE_3 on or off the QD tested. As shown in Figure 3, assembly of PTE_3 onto the QD caused an enhancement in catalytic activity compared to free enzyme at all the ratios tested for both QD sizes.

As shown in Table 1, the K_M values should be considered apparent values as the PTE_3/QD constructs are not the same as freely diffusing enzyme. The K_M values for our engineered PTE_3 are better or at least comparable to numerous other PTE wild types and variants but the k_{cat} is decreased.[19, 20] The highest apparent activity occurs at the lowest valency of PTE_3 on the smallest QD which we have noted before with alkaline phosphatase attached to QD. [18] The k_{cat} of PTE_3 attached to QD increased by 2X compared to PTE_3 free in solution at the lowest valency and smallest QD.

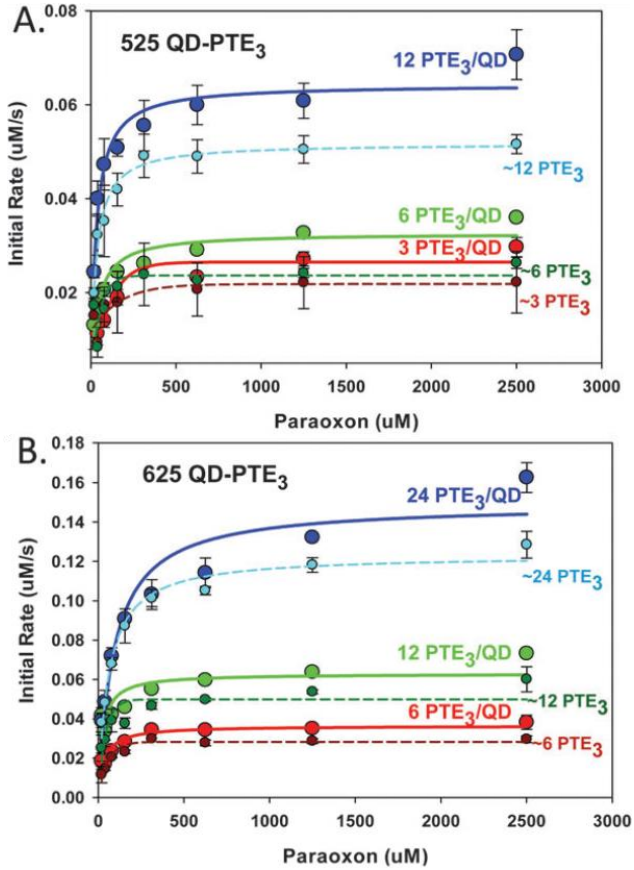

Figure 3. Trimeric PTE activity in solution and attached onto 525 nm (A) or 625 nm emitting QDs (B). Solid lines indicated activity of PTE when assembled onto QDs while dashed lines are equivalent amounts of free PTE in solution. Ratios or equivalents (~) of PTE to QD are indicated. Each data point is the average of three replicates. Note the difference in scale. Adapted from Ref. [15] with the permission of the Royal Society of Chemistry.

PTE_3/QD	k_{cat} (s^{-1})	K_M (μM)	k_{cat}/K_M ($\mu M^{-1}s^{-1}$)
525 nm QD			
3	7.9±1.0	111.9±18.9	0.07±0.01
6	4.9±0.3	33.3±7.7	0.15±0.03
12	4.8±0.4	30.0±6.9	0.16±0.03
Average:	5.9±1.8	58.4±11.2	0.13±0.05
625 nm QD			
6	5.1±0.8	28.8±1.8	0.18±0.03
12	4.7±0.1	24.6±3.3	0.19±0.02
24	5.7±0.6	167.1±39.5	0.05±0.03
Average:	5.2±0.5	73.5±20.3	0.14±0.07
PTE_3 alone			
Average:	3.9±0.8	50.1±9.8	0.10±0.03

Table 1: Summary of estimated PTE_3 kinetic parameters on or off QD. Adapted from Ref [15] with the permission of the Royal Society of Chemistry.

4 CONCULSIONS

By performing in-depth kinetic modeling we postulate an enhancement mechanism due to the substrate being captured by the bioconjugate and undergoing a translational diffusion process between closely-spaced enzymes on the QD surface. Another possibility is the solvation shell surrounding the PTE3/QD construct is influencing the kinetics. Development of these nanosensors as optical-based biosensors (e.g., within compact microfluidic devices) may greatly improve the sensitivity of conventional biological/chemical detection schemes. These enzyme/QD constructs have been engineered to have the substrate binding pocket facing outward, away from the QD surface thereby increasing favorable interactions with the substrate. Further work is being carried out to determine if these results can be replicated with other enzyme constructs and the influence of packing density as well as nanoparticle curvature in catalytic enhancement.

REFERENCES

[1] K. E. Sapsford *et al.*, "Analyzing Nanomaterial Bioconjugates: A Review of Current and Emerging Purification and Characterization Techniques," Analytical Chemistry, 83(12), 4453-4488 (2011).

[2] R. Gupta *et al.*, "Bacterial alkaline proteases: molecular approaches and industrial applications," Applied Microbiology and Biotechnology, 59(1), 15-32 (2002).

[3] B. J. Johnson, *et al.*, "Understanding enzymatic acceleration at nanoparticle interfaces: Approaches and challenges," Nano Today, 9(1), 102-131 (2014).

[4] E. Petryayeva, *et al.*, "Quantum Dots in Bioanalysis: A Review of Applications Across Various Platforms for Fluorescence Spectroscopy and Imaging," Applied Spectroscopy, 67(3), 215-252 (2013).

[5] J. Breger, *et al.*, "Continuing progress toward controlled intracellular delivery of semiconductor quantum dots," Wiley Interdisciplinary Reviews: Nanomedicine and Nanobiotechnology, (2014).

[6] K. Susumu, *et al.*, "Multifunctional Compact Zwitterionic Ligands for Preparing Robust Biocompatible Semiconductor Quantum Dots and Gold Nanoparticles," Journal of the American Chemical Society, 133(24), 9480-9496 (2011).

[7] J. B. Blanco-Canosa, *et al.*, "Recent progress in the bioconjugation of quantum dots," Coordination Chemistry Reviews, 263, 101-137 (2014).

[8] K. Susumu, *et al.*, "A New Family of Pyridine-Appended Multidentate Polymers As Hydrophilic Surface Ligands for Preparing Stable Biocompatible Quantum Dots," Chemistry of Materials, 26(18), 5327-5344 (2014).

[9] K. Boeneman, *et al.*, "Selecting Improved Peptidyl Motifs for Cytosolic Delivery of Disparate Protein and Nanoparticle Materials," Acs Nano, 7(5), 3778-3796 (2013).

[10] R. Walters, *et al.*, "Nanoparticle targeting to neurons in a rat hippocampal slice culture model," Asn Neuro, 4(6), (2012).

[11] B. K. Andrasfalvy, *et al.*, "Quantum dot-based multiphoton fluorescent pipettes for targeted neuronal electrophysiology," Nature Methods, 11(12), (2014).

[12] D. P. Dumas, *et al.*, "Purification and Properties of The Phopsphotriesterase From Pseudomonas-diminuta " Journal of Biological Chemistry, 264(33), 19659-19665 (1989).

[13] A. Yoshizumi, *et al.*, "Designed Coiled Coils Promote Folding of a Recombinant Bacterial Collagen," Journal of Biological Chemistry, 286(20), 17512-17520 (2011).

[14] A. Mohs, *et al.*, "Mechanism of stabilization of a bacterial collagen triple helix in the absence of hydroxyproline," Journal of Biological Chemistry, 282(41), 29757-29765 (2007).

[15] J. C. Breger, *et al.*, "Quantum dot display enhances activity of a phosphotriesterase trimer," Chemical Communications, (accepted), (2015).

[16] M. H. Stewart, *et al.*, "Competition between Forster Resonance Energy Transfer and Electron Transfer in Stoichiometrically Assembled Semiconductor Quantum Dot-Fullerene Conjugates," Acs Nano, 7(10), 9489-9505 (2013).

[17] T. L. Jennings, *et al.*, "Reactive Semiconductor Nanocrystals for Chemoselective Biolabeling and Multiplexed Analysis," Acs Nano, 5(7), 5579-5593 (2011).

[18] J. C. Claussen, *et al.*, "Probing the Enzymatic Activity of Alkaline Phosphatase within Quantum Dot Bioconjugates," Journal of Physical Chemistry C, 119(4), 2208-2221 (2015).

[19] C. J. Jackson, *et al.*, "Conformational sampling, catalysis, and evolution of the bacterial phosphotriesterase," Proceedings of the National Academy of Sciences of the United States of America, 106(51), 21631-21636 (2009).

[20] P. C. Tsai, *et al.*, "Enzymes for the Homeland Defense: Optimizing Phosphotriesterase for the Hydrolysis of Organophosphate Nerve Agents," Biochemistry, 51(32), 6463-6475 (2012).